Time-domain farfield scattering of plane acoustic waves by a penetrable object in the Born approximation

Dirk Quak, Adrianus T. de Hoop, and Hendrik J. Stam
Delft University of Technology, Department of Electrical Engineering, Laboratory of Electromagnetic Research, P. O. Box 5031, 2600 GA Delft, The Netherlands

(Received 29 July 1985; accepted for publication 11 June 1986)

The low-contrast or (first-order) Born approximation is applied to the time-domain scattering of a plane acoustic wave by a penetrable object of bounded extent embedded in a homogeneous fluid. Closed-form analytic expressions are obtained for the spherical-wave farfield scattering amplitude related to homogeneous objects of the following shapes: an ellipsoid, an elliptic cone of finite height, an elliptic cylinder of finite height, and a tetrahedron. Relaxation effects are included. The results are, amongst others, useful as test cases for time-domain inverse-scattering algorithms.

PACS numbers: 43.20.Fn

INTRODUCTION

In inverse scattering theory, much effort is put into the development of computer algorithms that ultimately are to reproduce the geometrical and/or physical parameters of unknown configurations from measured data pertinent to the scattered wave that results from a known wave incident on the unknown configuration to probe it.[1–10] In order to test these algorithms, often, at least in the initial phases, a linearized inversion scheme is used, based on the low-contrast or Born approximation. Further, an investigation in space–time seems the most appropriate one due to the fact that wave phenomena do take place in space–time. Hence, there is a need for analytical time-domain scattering results pertaining to simple, yet not too trivial, cases that can be used as test cases for computational time-domain inversion algorithms.

In the present paper, closed-form analytic expressions are derived for the spherical-wave, farfield, scattering amplitude in case a plane acoustic wave is incident upon a penetrable object of bounded extent situtated in a homogeneous surrounding fluid. Homogeneous objects of the following shapes are considered: an ellipsoid, an elliptic cone of finite height, an elliptic cylinder of finite height, and a tetrahedron. The analysis is carried out entirely in the space–time domain, and relaxation effects are included. A structure consisting of a composition of objects considered here can, in the Born approximation, be dealt with by superposition.

I. FORMULATION OF THE SCATTERING PROBLEM

In a homogeneous, unbounded fluid an acoustically penetrable, scattering object occupying the bounded domain $\mathscr{V}_1$ is present. The domain outside the object is denoted by $\mathscr{V}_0$ (Fig. 1). To locate position in space, we employ the coordinates $\{x,y,x\}$ with respect to an orthogonal Cartesian reference frame with origin O and three mutually perpendicular base vectors $\{\mathbf{i}_x,\mathbf{i}_y,\mathbf{i}_z\}$ of unit length each. These base vectors form, in the indicated order, a right-handed system. The position vector $\mathbf{r}$ is given by $\mathbf{r}=x\mathbf{i}_x+y\mathbf{i}_y+z\mathbf{i}_z$. The time coordinate is denoted by t. Partial differentiation is denoted by ∂ and $\nabla=\mathbf{i}_x\partial_x+\mathbf{i}_y\partial_y+\mathbf{i}_z\partial_z$. SI units are employed.

In $\mathscr{V}_0$ an ideal, homogeneous fluid is present. Its mechanical properties are characterized by the volume density of mass ρ_0 and the compressibility κ_0. In any source-free subdomain of $\mathscr{V}_0$ the acoustic wave quantities satisfy the linearized acoustic equations

$$\nabla p+\rho_0\partial_t\mathbf{v}=\mathbf{0}, \tag{1}$$

$$\nabla\cdot\mathbf{v}+\kappa_0\partial_t p=0. \tag{2}$$

The scattering object shows a contrast with respect to the surrounding fluid. This contrast is accounted for by the volume density of mass $\rho=\rho(\mathbf{r})$ and the compressibility relaxation function $\chi=\chi(\mathbf{r},t)$. Then, in $\mathscr{V}_1$, the acoustic wave quantities satisfy the equations

$$\nabla p+\rho(\mathbf{r})\partial_t\mathbf{v}=\mathbf{0}, \tag{3}$$

$$\nabla\cdot\mathbf{v}+\kappa_0\partial_t p+\kappa_0\partial_t\int_0^\infty\chi(\mathbf{r},\tau)p(\mathbf{r},t-\tau)d\tau=0. \tag{4}$$

In these equations, p denotes the acoustic pressure and $\mathbf{v}$ is the particle velocity. When the object is instantaneously reacting with the compressibility $\kappa(\mathbf{r})$, we have $\chi(\mathbf{r},t)=[\kappa(\mathbf{r})/\kappa_0-1]\delta(t)$. In Eq. (4), causality has been taken into account.

The object is irradiated by a uniform plane acoustic wave $\{p^i,\mathbf{v}^i\}$ with pressure amplitude p_0 and wave shape $a(t)$, and propagating in the direction of the unit vector α. The corresponding wavefunctions for p^i and $\mathbf{v}^i$ are given by

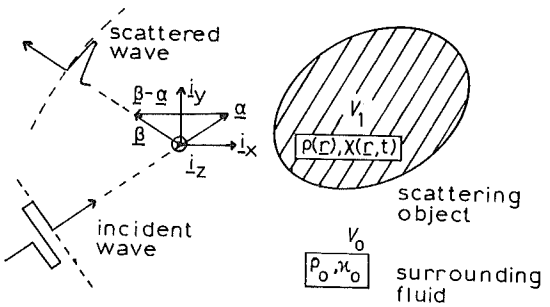

FIG. 1. Scattering configuration.

 0001-4966/86/101228-07$00.80

$$p^i = p_0 a(t - \boldsymbol{\alpha}\cdot\mathbf{r}/c_0) \tag{5}$$

and

$$\mathbf{v}^i = (\rho_0 c_0)^{-1} p_0 \boldsymbol{\alpha} a(t - \boldsymbol{\alpha}\cdot\mathbf{r}/c_0), \tag{6}$$

in which $c_0 = (\kappa_0 \rho_0)^{-1/2}$ is the acoustic wave speed in the surrounding fluid. The wave functions $\{p^s, \mathbf{v}^s\}$ for the scattered wave are defined as

$$p^s = p - p^i \text{ and } \mathbf{v}^s = \mathbf{v} - \mathbf{v}^i. \tag{7}$$

With Eqs. (1)–(7), it follows that p^s and $\mathbf{v}^s$ satisfy in $\mathbb{R}^3$ the equations

$$\nabla p^s + \rho_0 \partial_t \mathbf{v}^s = \mathbf{f}, \tag{8}$$

$$\nabla\cdot\mathbf{v}^s + \kappa_0 \partial_t p^s = \theta, \tag{9}$$

where

$$\mathbf{f} = -[\rho(\mathbf{r}) - \rho_0]\partial_t \mathbf{v} \tag{10}$$

is the contrast volume density of force and

$$\theta = -\kappa_0 \partial_t \int_0^\infty \chi(\mathbf{r},\tau) p(\mathbf{r}, t-\tau) d\tau \tag{11}$$

is the contrast volume density of injection rate. From Eqs. (8) and (9) it follows that $\{p^s, \mathbf{v}^s\}$ can be expressed as[11]

$$p^s(\mathbf{r},t) = \rho_0 \partial_t \psi - \nabla\cdot\mathbf{A}, \tag{12}$$

$$\mathbf{v}^s(\mathbf{r},t) = -\nabla\psi + \kappa_0 \partial_t \mathbf{A} + \rho_0^{-1} \nabla\times\left(\nabla\times\int_{-\infty}^t \mathbf{A}\, dt\right), \tag{13}$$

in which

$$\psi(\mathbf{r},t) = \int_{\mathbf{r}'\in\mathscr{V}_1} (4\pi|\mathbf{r}-\mathbf{r}'|)^{-1} \theta(\mathbf{r}', t - |\mathbf{r}-\mathbf{r}'|/c_0) dV \tag{14}$$

and

$$\mathbf{A}(\mathbf{r},t) = \int_{\mathbf{r}'\in\mathscr{V}_1} (4\pi|\mathbf{r}-\mathbf{r}'|)^{-1} \mathbf{f}(\mathbf{r}', t - |\mathbf{r}-\mathbf{r}'|/c_0) dV. \tag{15}$$

In the farfield region, Eq. (12) for the acoustic pressure reduces, with $\boldsymbol{\beta} = \mathbf{r}/|\mathbf{r}|$ as the unit vector in the direction of observation, to

$$p^s(\mathbf{r},t) \simeq (4\pi|\mathbf{r}|)^{-1} b(\boldsymbol{\beta}, t - |\mathbf{r}|/c_0) \tag{16}$$

and Eq. (13) for the particle velocity to

$$\mathbf{v}^s(\mathbf{r},t) \simeq (\rho_0 c_0)^{-1} (4\pi|\mathbf{r}|)^{-1} \boldsymbol{\beta} b(\boldsymbol{\beta}, t - |\mathbf{r}|/c_0), \tag{17}$$

with

$$b = b_{\text{mon}} + b_{\text{dip}}, \tag{18}$$

in which

$$b_{\text{mon}}(\boldsymbol{\beta},t) = \rho_0 \partial_t \int_{\mathbf{r}'\in\mathscr{V}_1} \theta(\mathbf{r}', t + \boldsymbol{\beta}\cdot\mathbf{r}'/c_0) dV \tag{19}$$

and

$$b_{\text{dip}}(\boldsymbol{\beta},t) = c_0^{-1} \partial_t \int_{\mathbf{r}'\in\mathscr{V}_1} \boldsymbol{\beta}\cdot\mathbf{f}(\mathbf{r}', t + \boldsymbol{\beta}\cdot\mathbf{r}'/c_0) dV. \tag{20}$$

In Eqs. (16) and (17) the delay in travel time from the origin, which is located near the scattering object, to the point of observation is included in the argument of b. It is clear that b_{mon} represents the monopole term and b_{dip} the dipole term.

Now, the scattering problem would have been solved if p and $\mathbf{v}$ were known in $\mathscr{V}_1$. For low-contrast scattering objects these quantities are in the (first-order) Born approximation replaced by the corresponding values of the incident wave. In the subsequent sections, this approximation will be carried out for a number of geometrical shapes.

II. THE BORN APPROXIMATION

In the low-contrast, or (first-order) Born approximation the unknown values of p and $\mathbf{v}$ in $\mathscr{V}_1$ are replaced by the known values of the incident wave functions p^i and $\mathbf{v}^i$, respectively. Then $b(\boldsymbol{\beta},t)$ changes into

$$b_{\text{mon}} = -c_0^{-2} p_0 \partial_t^2 \int_{\mathbf{r}'\in\mathscr{V}_1} dV \int_0^\infty d\tau \chi(\mathbf{r}',\tau) a(t - \tau + \mathbf{s}\cdot\mathbf{r}') \tag{21a}$$

and

$$b_{\text{dip}} = -c_0^{-2} p_0 (\boldsymbol{\beta}\cdot\boldsymbol{\alpha}) \partial_t^2 \int_{\mathbf{r}'\in\mathscr{V}_1} dV [\rho(\mathbf{r}')/\rho_0 - 1] \times a(t + \mathbf{s}\cdot\mathbf{r}'), \tag{21b}$$

where

$$\mathbf{s} = (\boldsymbol{\beta} - \boldsymbol{\alpha})/c_0. \tag{22}$$

In the further analysis, the right-hand sides of Eqs. (21a) and (21b) will be evaluated for a number of homogeneous objects of different shapes. Then, Eq. (21) can be written as

$$b_{\text{mon}} = -V p_0 \int_0^\infty \chi(\tau) \Upsilon(\mathbf{s}, t - \tau) d\tau, \tag{23a}$$

$$b_{\text{dip}} = -V p_0 (\boldsymbol{\beta}\cdot\boldsymbol{\alpha}) \Delta\rho \Upsilon(\mathbf{s},t), \tag{23b}$$

where V is the volume of the object, $\Delta\rho = (\rho/\rho_0 - 1)$ is the relative contrast in mass density, and

$$\Upsilon(\mathbf{s},t) = c_0^{-2} V^{-1} \int_{\mathbf{r}'\in\mathscr{V}_1} \partial_t^2 a(t + \mathbf{s}\cdot\mathbf{r}') dV \tag{24}$$

is a shape factor that depends on the shape and the dimensions of the objects, on the wave shape of the incident wave, and on $\mathbf{s}$. In the shape factor, the wave shape of the incident wave itself as well as its differentiated and integrated forms appear. For the differentiated wave shapes we employ the notation

$$D^n a = \partial_t^n a \quad \text{with } n = 1,2,\ldots. \tag{25}$$

The integrated wave shape is denoted by

$$Ia = \int_{-\infty}^t a(\tau) d\tau. \tag{26}$$

It follows immediately that when $\mathbf{s} = \mathbf{0}$ (i.e., for observation "behind" the object or "forward scattering"), we have

$$\Upsilon(\mathbf{0},t) = c_0^{-2} D^2 a(t), \tag{27}$$

which holds for any object.

Since $a(t + \mathbf{s}\cdot\mathbf{r})$ satisfies the equation $|\mathbf{s}|^{-2} \nabla\cdot\nabla a - \partial_t^2 a = 0$, when $\mathbf{s} \neq \mathbf{0}$, we can replace the operator $c_0^{-2}\partial_t^2$ by $|\mathbf{s}|^{-2} c_0^{-2} \nabla\cdot\nabla$ and apply Gauss' divergence theorem. This results, for Eq. (24), in the expression

$$\Upsilon(\mathbf{s},t) = |\mathbf{s}|^{-2}c_0^{-2}V^{-1}\int_{\mathbf{r}\in\partial\mathscr{V}_1}(\boldsymbol{\nu}\cdot\mathbf{s})Da(t+\mathbf{s}\cdot\mathbf{r})dA,$$
$$\text{when } \mathbf{s}\neq\mathbf{0}, \qquad (28)$$

where $\partial\mathscr{V}_1$ denotes the boundary of the scattering object and $\boldsymbol{\nu}$ is the unit vector along the outward normal to $\partial\mathscr{V}_1$. Equation (28) shows that the farfield, plane-wave scattering by a homogeneous object can, in the Born approximation, be viewed upon as a surface effect, when the observation is not "behind" the object [cf. Eq. (27)].

III. THE SHAPE FACTORS FOR THE DIFFERENT OBJECTS

In this section the shape factors for the ellipsoid, the elliptic cone of finite height, the elliptic cylinder of finite height, and the tetrahedron will be presented. Details of the calculation of these shape factors are given in the Appendixes.

A. Ellipsoid

For the ellipsoid defined by

$$\mathscr{V}_1 = \{\mathbf{r};0\leqslant x^2/a^2+y^2/b^2+z^2/c^2<1\}, \qquad (29)$$

the shape factor Υ is found to be

$$\Upsilon = (3c_0^{-2}/2\gamma^2)\{a(t+\gamma)+a(t-\gamma) - \gamma^{-1}[Ia(t+\gamma)-Ia(t-\gamma)]\}, \qquad (30)$$

where

$$\gamma = (s_x^2a^2+s_y^2b^2+s_z^2c^2)^{1/2}\geqslant 0. \qquad (31)$$

In the limiting case where $\gamma\to 0$, which corresponds to $\mathbf{s}\to\mathbf{0}$, the expression in the right-hand side of Eq. (30) reduces to the value $c_0^{-2}D^2a(t)$, which is in accordance with Eq. (27).

B. Elliptic cone of finite height

For the elliptic cone of finite height defined by

$$\mathscr{V}_1 = \{\mathbf{r};0\leqslant x^2/a^2+y^2/b^2<z^2/h^2, 0<z<h\}, \qquad (32)$$

the shape factor Υ is found to be

$$\Upsilon = (6/\pi c_0^2)\int_{-1}^{1}(\gamma\tau+s_zh)^{-2} \times\{(\gamma\tau+s_zh)Da(t+\gamma\tau+s_zh) - 2a(t+\gamma\tau+s_zh) + 2(\gamma\tau+s_zh)^{-1}[Ia(t+\gamma\tau+s_zh)-Ia(t)]\} \times(1-\tau^2)^{1/2}d\tau, \qquad (33)$$

where

$$\gamma = (s_x^2a^2+s_y^2b^2)^{1/2}\geqslant 0. \qquad (34)$$

For the limiting cases $s_z\to 0$, $\gamma\neq 0$ and $s_z\neq 0$, $\gamma\to 0$, the shape factor follows immediately from Eq. (33). In the case $\mathbf{s}\to\mathbf{0}$ (i.e., $\gamma\to 0$ and $s_z\to 0$), the shape factor follows from Eq. (33) as $\Upsilon = c_0^{-2}D^2a(t)$, which is in accordance with Eq. (27).

C. Elliptic cylinder of finite height

For the elliptic cylinder of finite height defined by

$$\mathscr{V}_1 = \{\mathbf{r};0\leqslant x^2/a^2+y^2/b^2<1, -h/2<z<h/2\}, \qquad (35)$$

the shape factor Υ is found to be

$$\Upsilon = (2/\pi c_0^2s_zh)\int_{-1}^{1}[Da(t+\gamma\tau+s_zh/2) - Da(t+\gamma\tau-s_zh/2)](1-\tau^2)^{1/2}d\tau, \qquad (36)$$

where

$$\gamma = (s_x^2a^2+s_y^2b^2)^{1/2}\geqslant 0. \qquad (37)$$

For the limiting case $s_z\to 0$, $\gamma\neq 0$, the shape factor Υ reduces to

$$\Upsilon = (2/\pi c_0^2)\int_{-1}^{1}D^2a(t+\gamma\tau)(1-\tau^2)^{1/2}d\tau. \qquad (38)$$

For the limiting case $\gamma\to 0$, $s_z\neq 0$, we have

$$\Upsilon = (1/c_0^2s_zh)[Da(t+s_zh/2)-Da(t-s_zh/2)]. \qquad (39)$$

The case $\mathbf{s}\to\mathbf{0}$ (i.e., $\gamma\to 0$ and $s_z\to 0$) follows either from Eq. (38) or Eq. (39) as $\Upsilon = c_0^{-2}D^2a(t)$, which is in accordance with Eq. (27).

D. Tetrahedron

For the tetrahedron defined by

$$\mathscr{V}_1 = \left\{\mathbf{r};\mathbf{r}=\sum_{n=1}^{4}\lambda_n\mathbf{r}_n, 0<\lambda_n<1, \sum_{n=1}^{4}\lambda_n=1\right\}, \qquad (40)$$

in which $\mathbf{r}_n$ denotes the position vector of vertex n ($n=1,2,3,4$), the shape factor Υ is found to be

$$\Upsilon = 6c_0^{-2}[(\gamma_{ij}\gamma_{ik}\gamma_{il})^{-1}Ia(t+\mathbf{s}\cdot\mathbf{r}_i) + (\gamma_{jk}\gamma_{jl}\gamma_{ji})^{-1}Ia(t+\mathbf{s}\cdot\mathbf{r}_j) + (\gamma_{kl}\gamma_{ki}\gamma_{kj})^{-1}Ia(t+\mathbf{s}\cdot\mathbf{r}_k) + (\gamma_{li}\gamma_{lj}\gamma_{lk})^{-1}Ia(t+\mathbf{s}\cdot\mathbf{r}_l)], \qquad (41)$$

in which

$$\gamma_{ij} = \mathbf{s}\cdot(\mathbf{r}_i-\mathbf{r}_j) = -\gamma_{ji}, \qquad (42)$$

and $\{i,j,k,l\}$ is a permutation of $\{1,2,3,4\}$.

As special cases we have to distinguish

(1) $\beta-\alpha$ is perpendicular to a single edge,

(2) $\beta-\alpha$ is perpendicular to two crossing edges,

(3) $\beta-\alpha$ is perpendicular to three edges (i.e., perpendicular to a face).

1. $\beta-\alpha$ perpendicular to a single edge

Let $\beta-\alpha$ be perpendicular to $\mathbf{r}_j-\mathbf{r}_i$ then $\gamma_{ij}=\gamma_{ji}=0$. The shape factor is now

$$\Upsilon = 6c_0^{-2}\{(\gamma_{ik}\gamma_{il})^{-1}[a(t+\mathbf{s}\cdot\mathbf{r}_i) - (\gamma_{ik}^{-1}+\gamma_{il}^{-1})Ia(t+\mathbf{s}\cdot\mathbf{r}_i)] + (\gamma_{ki}^2\gamma_{kl})^{-1}Ia(t+\mathbf{s}\cdot\mathbf{r}_k) + (\gamma_{li}^2\gamma_{lk})^{-1}Ia(t+\mathbf{s}\cdot\mathbf{r}_l)\}. \qquad (43)$$

2. $\beta-\alpha$ perpendicular to two crossing edges

Let $\beta-\alpha$ be perpendicular to $\mathbf{r}_j-\mathbf{r}_i$ and $\mathbf{r}_l-\mathbf{r}_k$, then $\gamma_{ij}=\gamma_{ji}=0$ and $\gamma_{kl}=\gamma_{lk}=0$. The shape factor is now

$$\Upsilon = 6c_0^{-2}\{\gamma_{ik}^{-2}[a(t+\mathbf{s}\cdot\mathbf{r}_i)+a(t+\mathbf{s}\cdot\mathbf{r}_k)] - 2\gamma_{ik}^{-3}[Ia(t+\mathbf{s}\cdot\mathbf{r}_i)-Ia(t+\mathbf{s}\cdot\mathbf{r}_k)]\}. \qquad (44)$$

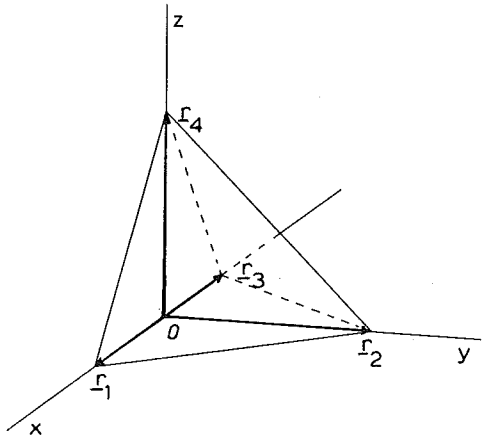

FIG. 2. Coordinate system and tetrahedron with vertices (1,0,0), (0,1,0), (− 1,0,0), and (0,0,1).

3. $\beta - \alpha$ perpendicular to three edges

Let $\beta - \alpha$ be perpendicular to $\mathbf{r}_j - \mathbf{r}_i$, $\mathbf{r}_k - \mathbf{r}_i$, and $\mathbf{r}_k - \mathbf{r}_j$, then $\gamma_{ij} = \gamma_{ji} = 0, \gamma_{ik} = \gamma_{ki} = 0$, and $\gamma_{jk} = \gamma_{kj} = 0$. The shape factor is now

$$\Upsilon = 6c_0^{-2}\{\gamma_{il}^{-3}[\tfrac{1}{2}\gamma_{il}^2 Da(t + \mathbf{s}\cdot\mathbf{r}_i) - \gamma_{il}a(t + \mathbf{s}\cdot\mathbf{r}_i) + Ia(t + \mathbf{s}\cdot\mathbf{r}_i)] + \gamma_{li}^{-3}Ia(t + \mathbf{s}\cdot\mathbf{r}_l)\}. \quad (45)$$

As before, $\{i,j,k,l\}$ is a permutation of $\{1,2,3,4\}$.

Finally, if $\mathbf{s} \to \mathbf{0}$ the shape factor follows from Eqs. (42)–(45) as $\Upsilon = c_0^{-2}D^2a(t)$, which is in accordance with Eq. (27).

IV. RESULTS

In this section we present some curves showing the shape factor as defined in Eq. (24) for a tetrahedron as a function of time. The location of the tetrahedron is given by its vertices $\mathbf{r}_1 = (1,0,0)$, $\mathbf{r}_2 = (0,1,0)$, $\mathbf{r}_3 = (-1,0,0)$ and $\mathbf{r}_4 = (0,0,1)$ (Fig. 2).

The tetrahedron is embedded in water ($\rho_0 = 1000$ kg/m^3, $c_0 = 1500$ m/s). A wave of unit amplitude and of wave shape (Fig. 3)

$$a(t) = \begin{cases} 0, & \text{when } -\infty < t < 0, \\ 1 - \cos(2\pi t/\Delta T), & \text{when } 0 < t < \Delta T, \\ 0, & \text{when } \Delta T < t < \infty, \end{cases} \quad (46)$$

is incident upon the tetrahedron. The duration ΔT of the pulse is taken as $\Delta T = 6.10^{-5}$ s. The duration of the pulse is chosen such that the influence of the position of the vertices shows up clearly. The direction of propagation of the incident wave is the positive y direction, i.e., $\alpha = (0,1,0)$. As directions of observation are chosen $(-\frac{1}{2}, -\frac{1}{2}, \frac{1}{2}\sqrt{2})$, $(0, -\frac{1}{2}\sqrt{2}, \frac{1}{2}\sqrt{2})$, $(0,0,-1)$, $(0,-1,0)$, and $(0,1,0)$, respectively, they illustrate the various cases characteristic for the tetrahedron.

In Fig. 4, the direction of observation and the direction of propagation of the incident wave are chosen such the $\beta - \alpha$ is not perpendicular to any edge. Then, the integrated form of the wave shape is present four times. In Fig. 5, $\beta - \alpha$ is perpendicular to a single edge. Correspondingly, the integrated form of the wave shape is present three times and the wave shape itself is present once. In Fig. 6, $\beta - \alpha$ is perpendicular to two crossing edges. Hence, the integrated form of the wave shape is present twice and the wave shape itself is also present two times. In Fig. 7, $\beta - \alpha$ is perpendicular to a face. Correspondingly, the differentiated form of the wave shape is present once, the wave shape itself is present once, and the integrated form of the wave shape is present two

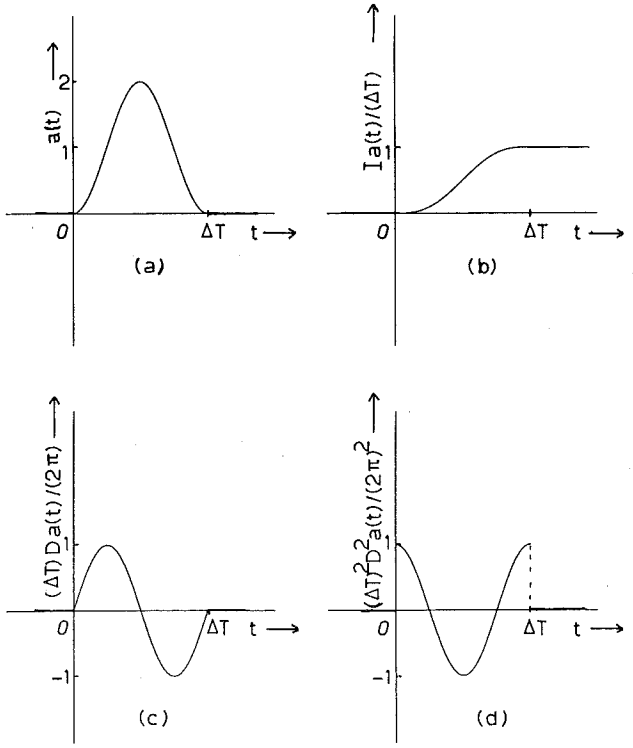

FIG. 3. Wave shapes related to the incident wave. (a) The wave shape itself; (b) its integrated form; (c) its differentiated form; (d) its twice differentiated form.

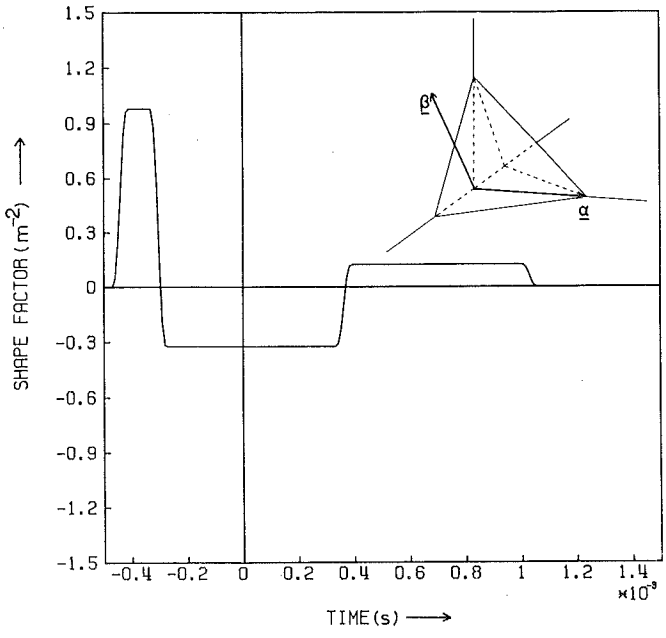

FIG. 4. Shape factor of the tetrahedron shown in Fig. 2 with $\beta = (-\frac{1}{2}, -\frac{1}{2}, \frac{1}{2}\sqrt{2})$, $\alpha = (0.1.0)$ (general case).

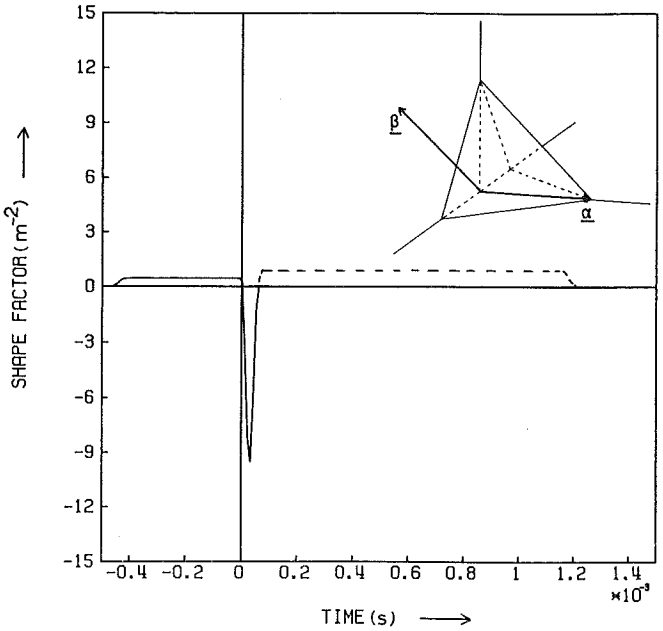

FIG. 5. Shape factor of the tetrahedron shown in Fig. 2 with $\beta = (0, -\frac{1}{2}\sqrt{2}, \frac{1}{2}\sqrt{2})$, $\alpha = (0,1,0)$ ($\beta - \alpha$ perpendicular to the edge $\mathbf{r}_3 - \mathbf{r}_1$). The amplitude in the dashed part of the curve is blown up by a factor of 10.

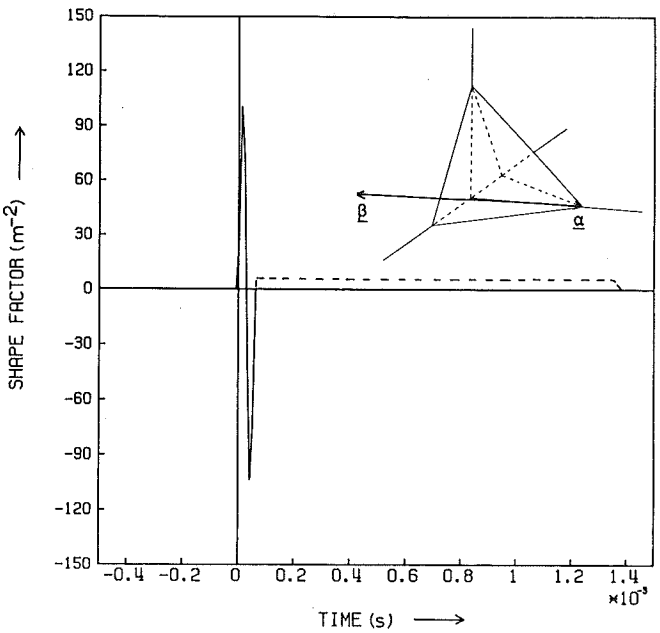

FIG. 7. Shape factor of the tetrahedron shown in Fig. 2 with $\beta = (0, -1, 0)$, $\alpha = (0,1,0)$ ($\beta - \alpha$ perpendicular to the face defined by the vertices $\mathbf{r}_1$, $\mathbf{r}_3$, and $\mathbf{r}_4$). The amplitude in the dashed part of the curve is blown up by a factor of 100.

times. In Fig. 8, $\beta - \alpha = 0$ (i.e., observation "behind" the object). Hence, only the two times differentiated wave shape is present.

Due to the very short duration of the pulse chosen such as to visualize the influence of the separate vertices, the amplitude of the integrated waveform is very small. In order to achieve the showing up of this amplitude in Figs. 5 and 7, its scale has been blown up by the factors of 10 and 100, respectively. Figure 7 shows that, in the first pulse, the differentiated waveform is predominant. Further, the wave shape itself manifests itself in the difference in amplitudes in the maximum and minimum, while the integrated wave shape is negligible.

V. CONCLUSION

With the aid of analytical techniques, expressions for the farfield acoustic pressure and particle velocity in a fluid have been derived, when a plane acoustic wave is incident upon a number of penetrable objects having a canonical ge-

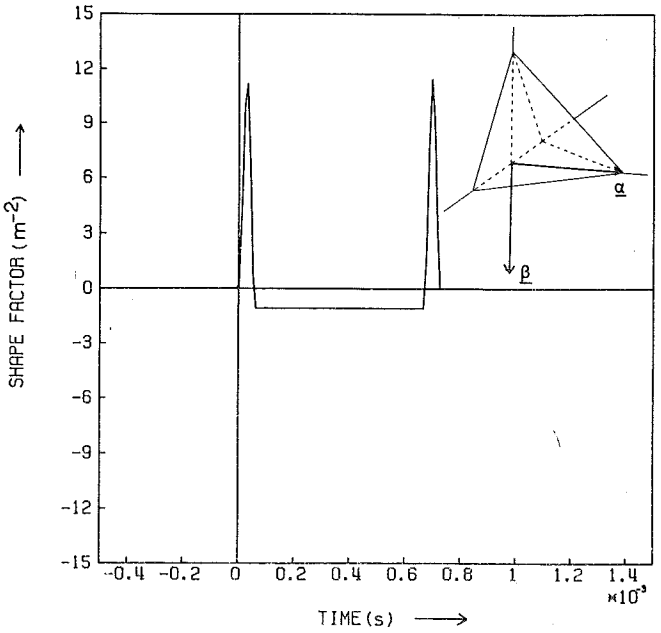

FIG. 6. Shape factor of the tetrahedron shown in Fig. 2 with $\beta = (0,0,-1)$, $\alpha = (0,1,0)$ ($\beta - \alpha$ perpendicular to the two crossing edges $\mathbf{r}_4 - \mathbf{r}_2$ and $\mathbf{r}_3 - \mathbf{r}_1$).

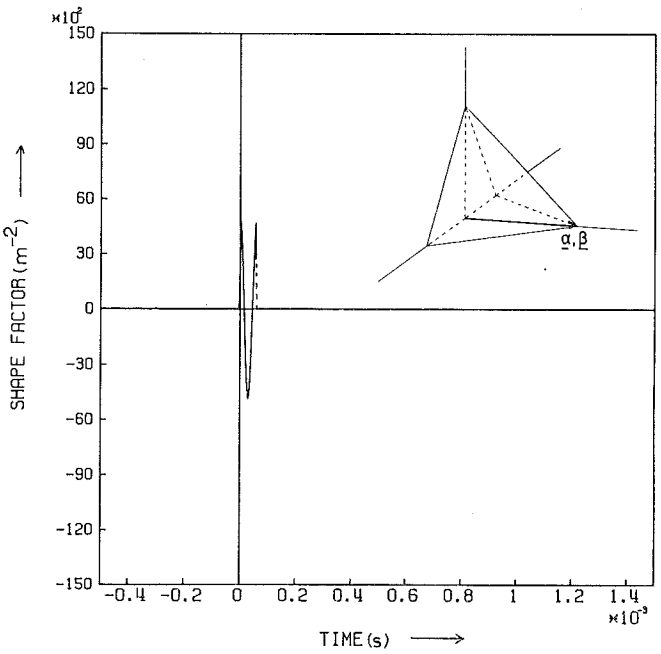

FIG. 8. Shape factor of the tetrahedron shown in Fig. 2 with $\beta = (0,1,0)$, $\alpha = (0,1,0)$ ($\beta - \alpha = 0$, i.e., forward scattering).

ometry. The numerical results for the shape factors of the tetrahedron illustrate the changes in wave shape that are observed in different directions. The synthetic data thus obtained for the simple, though not trivial, geometries can be used as test cases for computational time-domain inversion algorithms. This point of view has also been elaborated by Rose and Richardson[12] in connection with some examples of elastic-wave scattering.

APPENDIX A. CALCULATION OF THE SHAPE FACTOR OF THE ELLIPSOID

The ellipsoid is defined by Eq. (29). Its volume is given by

$$V = 4\pi abc/3. \tag{A1}$$

In order to perform the integration in the right-hand side of Eq. (24) we introduce as variables of integration

$$\xi = x/a, \quad \eta = y/b, \quad \zeta = z/c. \tag{A2}$$

In ξ, η, ζ space the domain of integration is the sphere $0 \leqslant \xi^2 + \eta^2 + \zeta^2 < 1$. By introducing in ξ, η, ζ space as variables of integration the polar coordinates $\{\rho,\theta,\phi\}$ with $0 \leqslant \rho < 1$, $0 \leqslant \theta \leqslant \pi$, $0 \leqslant \phi < 2\pi$, around $s_x a\mathbf{i}_x + s_y b\mathbf{i}_y + s_z c\mathbf{i}_z$ as axis, we obtain:

$$\mathbf{s}\cdot\mathbf{r} = (s_x a)\xi + (s_y b)\eta + (s_z c)\zeta = \gamma\rho\cos(\theta), \tag{A3}$$

where γ is given by Eq. (31), while

$$dV = abc\,\rho^2 \sin(\theta) d\rho\, d\theta\, d\phi. \tag{A4}$$

The integration in Eq. (24) is performed by replacing the differentiation of a with respect to t by differentiations with respect to the appropriate spatial variable of integration, and Eq. (30) results.

APPENDIX B. CALCULATION OF THE SHAPE FACTOR OF THE ELLIPTIC CONE OF FINITE HEIGHT

The elliptic cone of finite height is defined by Eq. (32). Its volume is given by

$$V = \pi abh/3. \tag{B1}$$

In order to perform the integration in the right-hand side of Eq. (24), we introduce as variables of integration

$$\xi = x/a, \quad \eta = y/b. \tag{B2}$$

In the ξ, η plane the domain of integration is the circle $0 \leqslant \xi^2 + \eta^2 < z^2/h^2$. By introducing in the ξ, η plane as variables of integration the polar coordinates $\{\rho,\theta\}$ with $0 \leqslant \rho < z/h$, $0 \leqslant \theta < 2\pi$ around $s_x a\mathbf{i}_x + s_y b\mathbf{i}_y$ as axis we obtain:

$$\mathbf{s}\cdot\mathbf{r} = (s_x a)\xi + (s_y b)\eta + s_z z = \gamma\rho\cos(\theta) + s_z z, \tag{B3}$$

where γ is given by Eq. (34), while

$$dx\,dy\,dz = ab\,\rho d\rho\, d\theta\, dz. \tag{B4}$$

The integration in Eq. (24) is performed by replacing the differentiation of a with respect to t by differentiations with respect to the appropriate spatial variable of integration. Further, the integral with respect to θ is reduced to one over the interval $(0,\pi)$ and $\tau = \cos(\theta)$ is introduced as variable of integration. The final result, Eq. (33), is obtained by performing consecutively the integration with respect to ρ, an integration by parts with respect to τ and, finally, the integration with respect to z.

APPENDIX C. CALCULATION OF THE SHAPE FACTOR OF THE ELLIPTIC CYLINDER OF FINITE HEIGHT

The elliptic cylinder of finite height is defined by Eq. (35). Its volume is given by

$$V = \pi abh. \tag{C1}$$

In order to perform the integration in the right-hand side of Eq. (24), we introduce as variables of integration

$$\xi = x/a, \quad \eta = y/b. \tag{C2}$$

In the ξ, η plane the domain of integration is the circle $0 \leqslant \xi^2 + \eta^2 < 1$. By introducing in this ξ, η plane as variables of integration the polar coordinates $\{\rho,\theta\}$ with $0 \leqslant \rho < 1$, $0 \leqslant \theta < 2\pi$ around $s_x a\mathbf{i}_x + s_y b\mathbf{i}_y$ as axis we obtain

$$\mathbf{s}\cdot\mathbf{r} = (s_x a)\xi + (s_y b)\eta + s_z z = \gamma\rho\cos(\theta) + s_z z, \tag{C3}$$

where γ is given by Eq. (37), while

$$dx\,dy\,dz = ab\,\rho d\rho\, d\theta\, dz. \tag{C4}$$

The integration in Eq. (24) is performed by replacing the differentiations of a with respect to t by differentiations with respect to the appropriate spatial variable of integration. First, the integration with respect to z is performed, which is elementary. Further, the integral with respect to θ is reduced to one over the interval $(0,\pi)$ and $\tau = \cos(\theta)$ is introduced as variable of integration. The final result, Eq. (36), is obtained by performing an appropriate integration by parts with respect to τ.

APPENDIX D. CALCULATION OF THE SHAPE FACTOR OF THE TETRAHEDRON

The tetrahedron is defined by Eq. (40). Its volume is given by

$$V = |\{\mathbf{r}_l - \mathbf{r}_i)\cdot[(\mathbf{r}_j - \mathbf{r}_i)\times(\mathbf{r}_k - \mathbf{r}_i)]/6\}|, \tag{D1}$$

in which $\{i,j,k,l\}$ is a permutation of $\{1,2,3,4\}$.

In Eq. (40) λ_1, λ_2, λ_3, and λ_4 denote the barycentric coordinates of a point in the interior or on the boundary of the tetrahedron. In order to perform the integration in the right-hand side of Eq. (24), we replace λ_1 by $1 - \lambda_2 - \lambda_3 - \lambda_4$ and carry out the integration over the ranges $0 < \lambda_2 < 1$, $0 < \lambda_3 < 1 - \lambda_2$, $0 < \lambda_4 < 1 - \lambda_2 - \lambda_3$. Further, we take into account the value of the Jacobian $\partial(x,y,z)/\partial(\lambda_2,\lambda_3,\lambda_4) = 6V$. The integration in Eq. (24) is performed by replacing the differentiation of a with respect to t by differentiations with respect to λ_2, λ_3 or λ_4. The special cases are most easily dealt with by redoing the integrations that need modification.

[1] D. Miller, M. Oristaglio, and G. Beylkin, "A new formalism and an old heuristic for seismic migration," Extended Abstracts, 54th Annual Meeting of the SEG, Atlanta (1984).

[2] G. Beylkin, "Imaging of discontinuities in the inverse scattering problem by inversion of a causal generalized Radon transform," J. Math. Phys. **26**, 99–108 (1985).

[3] Y. Das and W.-M. Boerner, "On radar target shape estimation using algorithms for reconstruction from projections," IEEE Trans. Antennas Propagat. **AP-26**, 274–279 (1978).

[4]W.-M. Boerner, C. M. Mo, and B. Y. Foo, "Use of Radon's projection theory in electromagnetic inverse scattering," IEEE Trans. Antennas Propagat. **AP-29**, 336–341 (1981).
[5]W.-M. Boerner and C. M. Mo, "Analysis of physical optics far-field inverse scattering for the limited data case using Radon theory and polarization information," Wave Motion **3**, 311–333 (1981).
[6]J. H. Rose and J. L. Opsal, "The inverse Born approximation: exact determination of shape of convex voids," in *Review of Progress in Quantitative Nondestructive Evaluation*, edited by D. O. Thompson and D. E. Cimenti (Plenum, New York, 1983), pp. 949–959.
[7]J. H. Rose, M. Cheney, and B. DeFacio, "The connection between time- and frequency-domain three-dimensional inverse scattering methods," J. Math. Phys. **25**, 2995–3000 (1984).
[8]N. N. Bojarski, "Three dimensional electromagnetic short pulse inverse scattering," Syracuse Univ. Research Corp., Syracuse, N.Y., Special Projects Lab. Rep. No. SURC SPL 67-3 NTIS # AD/845126 (Feb. 1967).
[9]N. N. Bojarski, "Electromagnetic inverse scattering theory," Syracuse Univ. Research Corp., Syracuse, N.Y., Special Projects Lab. Rep. No. SURC SPL R68-70 NTIS # AD/509134 (Dec. 1968).
[10]N. N. Bojarski, "Electromagnetic inverse scattering," Naval Air Systems Command Contract N00019-72-0-0462 Rep. (June 1972).
[11]A. T. de Hoop, "A time-domain energy theorem for scattering of plane acoustic waves in fluids," J. Acoust. Soc. Am. **77**, 11–14 (1985).
[12]J. H. Rose and J. M. Richardson, "Time domain Born approximation," J. Nondestructive Evaluation **3**, 45–53 (1982).